Synthesis and Characterization of Emulsion Polymerized Mixed Matrix Aluminum Silicate/Poly(2,6-dimethyl 1,4-phenylene oxide) Films

F. Sadeghi, A. Y. Tremblay, B. Kruczek

Department of Chemical Engineering, University of Ottawa, 161 Louis Pasteur, Ottawa, Ontario, Canada K1N 6N5

Received 30 August 2007; accepted 20 December 2007
DOI 10.1002/app.28296
Published online 18 April 2008 in Wiley InterScience (www.interscience.wiley.com).

ABSTRACT: A series of poly (2,6-dimethyl-1,4-phenylene oxide) (PPO)-based organic/inorganic films for the potential application in membrane gas separation were prepared by employing a method in which aluminum hydroxonitrate contained in a stable water-in-oil (W/O) emulsion, the oil phase being a solution of PPO in trichloroethylene, was mixed with a homogeneous solution of PPO in trichloroethylene containing tetraethyl orthosilicate (TEOS). Inorganic polymerization occurred in or at the surface of the aqueous droplets of the W/O emulsion. Subsequently, thin films were prepared by a spin coating technique, and they were referred to as emulsion polymerized mixed matrix (EPMM) films. Scanning electron micrographs taken from a film cross section indicated the presence of particles in the PPO matrix, and energy dispersive X-ray measurements showed that the embedded particles contained Al and Si elements. Differential scanning calorimetry analysis showed a decrease in the glass transition of the EPMM films with increase of TEOS loading. The compatibility between aluminum silicate nanoparticles and PPO in the EPMM films was confirmed by air separation tests. © 2008 Wiley Periodicals, Inc. J Appl Polym Sci 109: 1454–1460, 2008

Key words: poly(2,6-dimethyl-1,4-phenylene oxide); W/O emulsion; aluminum silicate; spin coating; gas separation membranes

INTRODUCTION

The incorporation of inorganic materials into polymer matrices has been a promising strategy to improve the transport and thermal properties of polymeric films.[1] Mixed matrix films are composite materials where inorganic components such as zeolites or molecular sieves are dispersed in a polymer matrix. These films are to combine properties of the both materials, i.e., the selectivity of zeolites and the ease of processing of polymeric films and consequently they might be very useful for membrane gas separation.[2,3] The interaction between polymer chains and inorganic particles is a controlling factor in manufacturing the mixed matrix films. Weak interaction between two materials causes the formation of voids at the inorganic/organic interface, which ultimately results in nonselective passing of penetrants through these voids.[4,5]

To promote a good dispersion of inorganic phase in polymers, the simplest method is to grow the inorganic phase by a sol–gel process in a polymer solution, which leads to so-called hybrid materials.[6] For the preparation of the inorganic phase, a silica alkoxide such as tetraethyl orthosilicate (TEOS) or tetramethyl orthosilicate (TMOS) is added to a polymer solution and hydrolysis and condensation of the silica alkoxide is induced by acid catalysis.[7–10] The compatibility between the polymer and inorganic phases plays a major role in the properties of the hybrid materials. When there is no compatibility between the inorganic phase and the polymer chains the incorporation of inorganic materials in the polymer matrix leads to phase separation.[11] The compatibility of phases in hybrid materials is enhanced by formation of hydrogen or covalent bonding between the two phases. Some polymers such as poly(vinyl acetate), poly(vinylpyrrolidone) are able to form hydrogen bonds with a silanol on silicate networks,[12] whereas polymers such as polyimide can form covalent bonds between the inorganic and organic segments.[13–15] Another procedure for forming hydrogen bonding in hybrid materials is to functionalize the polymer structure with trialkoxysilyl groups. This functionalized polymer then polymerizes via a sol–gel process with adding a coupling agent.[16] So far all studies on these hybrid materials have focused on the formation of silica in polymer solutions by hydrolysis and condensation of silicon alkoxides by acid catalysis.

In this study, we have developed a new category of films, which will be referred to as emulsion

Correspondence to: B. Kruczek (bkruczek@uottawa.ca).
Contract grant sponsor: Natural Science and Engineering Research Council of Canada.

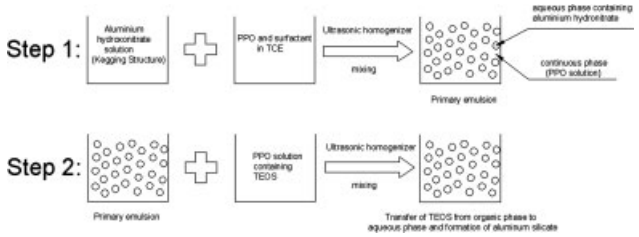

Figure 1 The schematic diagram of the procedure for the preparation W/O emulsion.

polymerized mixed matrix (EPMM) films. To prepare these films we have explored a new method, in which an inorganic precursor contained in a stable W/O emulsion is allowed to polymerize in the continuous phase of a polymer solution. The aqueous phase was used as a micro-reactor for growing the inorganic phase. The inorganic particles were formed by the copolymerization of TEOS and aluminum hydroxide in an aqueous phase emulsified in a dilute solution of poly (2,6-dimethyl-1,4-phenylene oxide) in trichloroethylene. These emulsions were used for the preparation of thin films using a spin coating technique.

EXPERIMENTAL

Materials

Poly(2,6-dimethyl-1,4-phenylene oxide), PPO, with an intrinsic viscosity 1.78 dL/g in chloroform at 25°C was supplied by GE Plastics (Selkirk, NY, USA). Tetraethyl orthosilicate (TEOS, reagent grade 98%), aluminum nitrate nonahydrate (98+% A.C.S. reagent), sodium carbonate anhydrous (granular, A.C.S. reagent), *N*-octanol (99+%, HLB = 5.1), and trichloroethylene (TCE, 99.5% + A.C.S. reagent) were purchased from Sigma Aldrich (Oakville, ON, Canada). All chemicals were used as received.

EPMM film preparation

The two steps involved in the preparation of EPMM films are described below.

Preparation of spin coating solutions

A W/O emulsion was used to prepare a spin coating solution. It was prepared in a two-step procedure as shown in Figure 1. The aluminum hydroxonitrate solution required for the first step as prepared by first dissolving aluminum nitrate in deionized water and then adding into it sodium carbonate solution. The concentrations of aluminum nitrate, $Al(NO_3)_3 \cdot 9H_2O$, and sodium carbonate in the resultant solution were 0.375 and 0.107 g/cm^3, respectively.

The above composition of the aqueous phase was determined in parallel experiments, in which the effect of concentration of sodium carbonate on polymerization of TEOS in the presence of aluminum hydroxonitrate was investigated. Since TEOS is not soluble in aqueous aluminum hydroxonitrate solution, a mutual solvent – ethanol had to be used. The volume ratio of TEOS : ethanol : aluminum hydroxonitrate solution was maintained constant at 1 : 3 : 1 while the amount of sodium carbonate was varied. Following the study of Eliseev et al.,[17] copolymerization of TEOS and aluminum hydroxonitrate was assessed on the basis of a gelation time and the appearance of the formed gel.

The aluminum hydroxonitrate solution containing optimized amount sodium carbonate was dispersed in 5 cm^3 of 10% PPO solution in TCE containing *N*-octanol as a surfactant, and sonicated using an ultrasonic homogenizer (Fischer Scientific, Model 550, Pittsburgh, PA) for a specific time, depending on the volume fraction of the aqueous phase. In the second step, the primary emulsion was added to 5 cm^3 of 10% PPO solution in TCE containing TEOS, and stirred using the ultrasonic homogenizer for a specific time depending on the TEOS loading. Quantities of the ingredients used for the preparation of the primary and secondary emulsions along with the ultrasound energy density applied in each step are shown in Table I.

Film preparation

Spin coating solution (10 cm^3) was placed on a silicone wafer (4 in. diameter) and spun at 600 rpm for 200 s. This formed a smooth film on the surface of the wafer. The coated wafer was kept at room

TABLE I
Spin Coating Solutions for Preparation of EPMM Films

	Primary emulsion			Secondary emulsion	
Solution	Fraction volume of aqueous solution (%)	*N*-Octanol (vol %)	Energy density (kJ/cm^3)	TEOS[a] (wt %)	Energy density (kJ/cm^3)
EPMM1	0.34	0.21	1.8	5	7.56
EPMM2	0.69	0.42	3.6	10	32.4

[a] Based on the mass of the polymer

temperature for 2 h after which it was placed in a vacuum oven. The oven with the film inside was purged with nitrogen followed by its evacuation to remove oxygen trace from air. The purging-evacuation cycle was repeated four times after which the vacuum oven was set at 120°C and maintained at this temperature for 2 h. Following this, the heating was turned off and the vacuum oven was let to cool to ambient temperature. A second layer was applied by delivering another 10 cm^3 of the spin coating solution, over the rotating wafer with the first layer, at 600 rpm and spinning it for 200 s, after which the wafer was kept at ambient temperature for 2 h. The second coating was applied over the wafer while it was rotating to prevent the dissolution of the first coat. This dissolution occurred when fresh solution was allowed to rest on the surface of the coated wafer for even a few seconds. The addition of the second coat while the wafer was rotating produced a film of uniform thickness across the diameter of the wafer. The film was then peeled off the wafer by soaking it in deionized water for 5 min. The unreacted TEOS was washed out from the free-standing film by boiling it in deionized water for 4 h. Finally, the film was dried in a vacuum oven, which was purged with nitrogen as described above, at 120°C for 2 days. The thickness of such prepared EPMM films was ranging from 13 and 16 μm.

For comparison, blank PPO films were prepared by placing 10 cm^3 of 10% PPO solution in TCE on the wafer and spun at 600 rpm for 200 s. The coated wafer was dried and heated in the vacuum oven as described above after which another 10 cm^3 of the PPO solution was applied on the wafer coated with the first layer, which was rotating at 600 rpm, and spun for 200 s. After peeling off the film from the wafer using deionized water the free standing film was dried and heated in the vacuum oven at 120°C for 2 days, as described above.

Characterization

The aqueous droplet size of the primary emulsion of the spin coating solutions was measured using a dynamic light scattering (DLS) instrument (Malvern Zetasizer, UK). The mean droplet size, expressed as the Sauter diameter,[18] was calculated from the DLS measurements using the following equation:

$$d_{32} = \frac{\sum_{i=1}^{N} n_i d_i^3}{\sum_{i=1}^{N} n_i d_i^2} \quad (1)$$

where: d_{32} is the Sauter diameter, n_i is the number of droplets, and d_i is the droplet size.

The X-ray diffraction spectra of the synthesized films were obtained using an X-ray Diffractometer (SCINTAG, Model 2000, Cupertino, CA). The spectra were obtained using a step size of 0.020° over a 2θ range of 2° to 40°.

A TGA2950 thermoanalysis instrument (TA Instruments, New Castle, DE) was used to investigate the degradation process and thermal stability of the films. The TGA measurements were carried out under nitrogen with a scanning rate of 10°C/min from 25° to 800°C. Differential scanning calorimetry (DSC) was performed using a QA series TA 1000 differential scanning calorimetric analyzer (TA Instruments) equipped with a cooling apparatus. The heating rate was 10°C/min from 40° to 250°C, and nitrogen flow was 50 mL/min.

The film cross section was investigated using a Hittachi S3200N scanning electron microscope (SEM) (Hittachi, Pleasanton, CA) instrument equipped with an Oxford LINK ISIS energy dispersive X-ray (EDX) spectrometer.

Gas transport properties of films were determined in air separation experiments performed in a constant pressure testing system equipped with a gas chromatography (GC) unit. The system consisted of two permeation test cells having the permeation area of 20 cm^2 each. An HP 5700 gas chromatograph, with a thermal conductivity detector and a 5 Å molecular sieve column, was used to measure the composition of the feed and permeate streams. The tests were performed at a feed pressure of 414 kPa with the retentate flow rate set to 110 cm^3/min; the retentate and permeate streams were discharged to atmosphere. The volumetric flow rate of the permeate stream was measured by a bubble flow meter.

To obtain quantitative results from the GC, a thermal correction was applied to the GC spectra. The thermal response values for oxygen and nitrogen are 40 and 42, respectively.[19] Normalized GC peaks were obtained by dividing the actual area of the GC response peaks by the respective thermal response values of the components, and then the mole fractions of the components was obtained by using these normalized peaks.

The separation factor (α) for a pair of gases i and j was obtained by:

$$\alpha_{ij} = \frac{y_i/y_j}{x_i/x_j} \quad (2)$$

where y and x refer to the mole fractions in the permeate and feed streams, respectively. The permeability coefficient of gas i (P_i) was calculated using the following correlation[20]:

$$P_i = \frac{Q_i l}{A \Delta p_i} \quad (3)$$

where Q_i is a steady state permeation rate of gas i determined from the total permeate flow and its composition, l is a film thickness, A is a permeation area of the film, and Δp_i is a difference of the partial pressures of component i across the film. The ideal selectivity for components i and j (α^*_{ij}) can be calculated from the respective permeability coefficients evaluated from eq. (3). Alternatively, the ideal selectivity can be calculated from the separation factor using the following correlation[21]:

$$\alpha^*_{ij} = \alpha_{ij} \Big/ \left(\frac{x_i(\alpha_{ij} - 1) + 1 - r\alpha_{ij}}{x_i(\alpha_{ij} - 1) + 1 - r} \right) \quad (4)$$

where r is the ratio of the downstream pressure to the upstream pressure.

RESULTS AND DISCUSSION

Characterization of W/O emulsion

The important parameters for a W/O emulsion used in preparation of EPMM films are: the degree of hydrolysis of the aluminum hydroxonitrate inside the internal aqueous phase of W/O emulsion, and the size of the aqueous droplets.

Copolymerization of TEOS and aluminum hydroxonitrate requires tetrahedrally coordinated aluminum in the aqueous solution. Eliseev et al. showed that the rates of hydrolysis and condensation polymerization of TEOS in the presence of aluminum hydroxonitrate increases significantly in the system when the degree of hydrolysis of the aluminum nitrate is higher than 1.9 and aluminum is in a tetrahedral form.[17] The rapid hydrolysis of TEOS in the presence of aluminum hydroxonitrate in ethanol media leads to a short gelation time. On the contrary, slow hydrolysis of TEOS leads to a long gelation time, which indicates a low degree of aluminum hydroxonitrate hydrolysis. In the present study, the minimum gelation time ranging from 4 to 7 min for the hydrolysis and condensation of TEOS in the presence of aluminum hydroxonitrate in ethanol media was observed when the concentration of sodium carbonate in the resultant solution was 0.107 g/cm^3. According to Eliseev et al. such sort gelation times indicate that the degree of hydrolysis of aluminum hydroxonitrate was greater than 1.9 and aluminum was tetrahedrally coordinated.[17]

A W/O emulsion prepared as described above, contained *N*-octanol, which has an HLB of 5.1.[22] Consequently, *N*-octanol acts as an oil-soluble surfactant. Table II shows the Sauter diameter, obtained from the DLS measurements, of the internal aqueous droplets in the W/O emulsions used in the preparation of EPMM1 and EPMM2 films along with the energy density used in the first step of the W/O emulsion preparation.

It can be observed from this table that doubling of the energy density in preparation of the emulsion, containing twice the amount of the aqueous phase, did not maintain the size of the emulsion at the value of 245 nm (observed in the W/O emulsion used in the preparation of the EPMM1 membrane). This can be due to a high viscosity of the continuous phase (10% PPO solution). At a higher aqueous phase content, the possibility of droplet coalescence increases. This will be enhanced by a viscous nature of the continuous phase. After disruption, the droplets are slowly separated; this increases their contact time and favors coalescence.[23]

X-ray diffraction spectra

The wide-angle X-ray patterns obtained from the EPMM1 and EPMM2 films are compared with those of the blank PPO film and aluminum silicate powder in Figure 2. The X-ray spectrum of the PPO film shows a major peak occurring at $2\theta = 14.28^\circ$, which corresponds to a *d*-spacing of 6.2 Å. This *d*-spacing value is in agreement with 6.1 Å reported by Story and Koros for a PPO film.[24] In addition, a broad peak is present at $2\theta = 28.6^\circ$, which corresponds to a *d*-spacing of 3.1 Å. The X-ray spectrum of the aluminum silicate powder shows that the aluminum silicate powder prepared at low temperature has an amorphous domain, which is consistent with the result reported by Huang et al. [25] A sharp X-ray diffraction peak indicates that a polymer contains crystalline domains, whereas an amorphous polymer is characterized by a broad X-ray diffraction peak.[26] Although the X-ray measurements of EPMM1 and EPMM2 films show that the locations of the peaks are not changed by the incorporation of aluminum silicate, the normalized intensity of the major peak

TABLE II
Sauter Diameter of the Internal Aqueous Droplet Along Energy Density Applied for the Preparation of the W/O Emulsion

W/O emulsions	Internal aqueous phase volume content (%)	Sauter diameter (nm)	St. Dev	Energy density (kJ/cm^3)
EPMM1	0.34	245	10.2	1.8
EPMM2	0.69	344	16.1	3.6

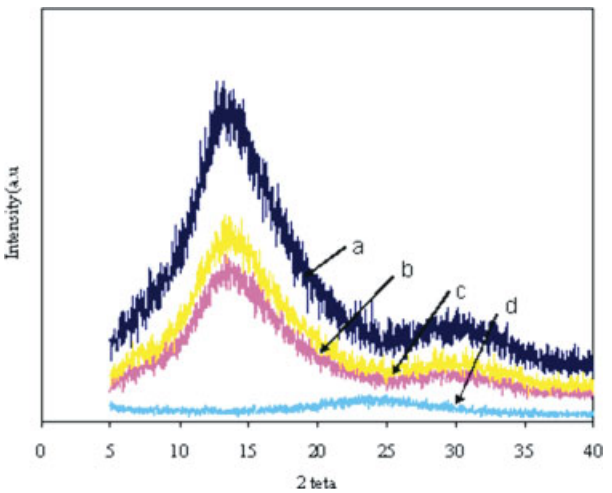

Figure 2 Normalized X-ray diffraction spectra of (a) blank PPO, (b) EPMM1, (c) EPMM2 films and (d) aluminum silicate powder. [Color figure can be viewed in the online issue, which is available at www.interscience.wiley.com.]

in EPMM1 and EPMM2 are reduced compared to the blank PPO by 44.2% and 51.7%, respectively. The X-ray spectra of EPMM1 and EPMM2 are typical of amorphous materials. This is consistent with the results reported by Zhang et al.,[27] who modified PPO by incorporation of silica into the polymer structure through a sol–gel process. Similar results are also reported for other polymers modified by incorporation of silica.[28] Using X-ray diffraction analysis, Kim and Lee observed that the crystallinity of poly(amide-6-*b*-ethylene oxide) decreases with increasing inorganic (TEOS) content. Also, Kim et al.[29] reported that X-ray diffraction peaks of poly (vinyl alcohol)/SiO_2 hybrid film become somewhat broadened with increasing the silica content.

Thermal analysis

Thermogravimetric (TG) analysis and differential scanning calorimetry (DSC) were carried out on the films to determine their decomposition temperature, glass transition temperature, and an inorganic content. Table III presents the results of the TG analysis of the PPO and EPMM2 films. A decomposition temperature of 480°C was observed for the PPO film, which is comparable to the value of 456°C reported by Karasz and O'Reilly[30] and the value of 464°C reported by Tran and Kruczek.[31] The decomposition temperature of the EPMM2 film occurred at around 495°C, which indicates an improvement in thermal stability compared to the blank PPO film. This agrees with a general statement that the incorporation of inorganic components into polymers improves their thermal stability.[32] In the EPMM2 film, the residual weight after the polymer decomposition indicates the presence of an inorganic content. At 700°C, the residual weight percentage for EPMM2 was 2.57 whereas the residual weight percentage for the PPO film was 0.45, which is attributed to PPO impurities. From the difference between the residual weight percentage of the EPMM2 and PPO films it can be concluded that the conversion with respect to SiO_2 is around 71.6%.

TABLE III
The Results of TG Analysis of Blank PPO and EPMM2 Films

Films	TEOS (wt %)	SiO_2 (wt %)	ash (wt %)	T_d (°C)
Blank PPO	0	0	0.45	480
EPMM2	10	2.88	2.57	495

The DSC measurements were performed to investigate the effect of the inorganic loading on the glass transition temperature (T_g) of the films. As is shown in Figure 3, the respective T_g of EPMM1 and EPMM2 films, which correspond to 5 and 10% of the inorganic loading based on TEOS, are 204.0 and 182.5°C, respectively. In contrast, the blank PPO film has T_g equal to 217.5°C. A decrease in the glass transition temperature indicates that the presence of inorganic particles reduce the rigidity of the of the polymer chains.

Scanning electron microscopy

The SEM image taken from a cross section of the EPMM2 film along with the EDX-analysis is shown in Figure 4. The SEM image of the cross section of the EPMM2 film shows the presence of particles in the PPO structure. On the other hand, the EDX analyses indicate that these particles contain both Al and Si elements, which confirms that the hydrolysis and condensation of TEOS was induced by the aluminum hydroxonitrate.

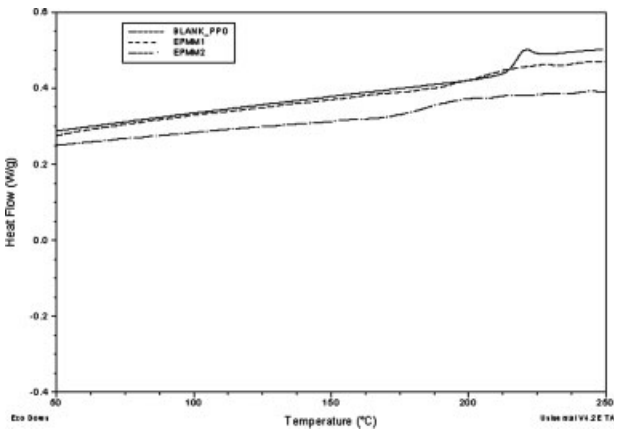

Figure 3 DSC of blank PPO, EPMM1, and EPMM2 films. Second heating run used for the determination of glass transition temperature of the films.

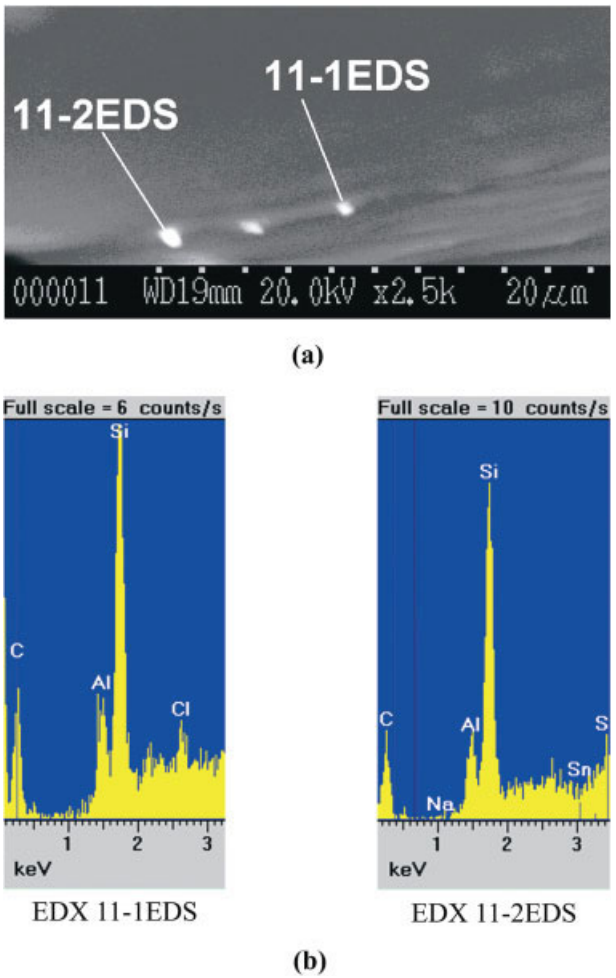

Figure 4 SEM image and EDX spectrum of the EPPM2 film cross section: (a) SEM image with magnification 2500; (b) EDX spectrum of the 11-1EDS and 11-2EDS particles. [Color figure can be viewed in the online issue, which is available at www.interscience.wiley.com.]

Air separation tests

A summary of the results obtained from air separation tests with the blank PPO and EPMM films is presented in Table IV. The average and the standard deviation values for the separation factor, ideal selectivity, and permeability coefficient were determined when the system reached steady state based on at least seven data points gathered over at least 20 h. The standard deviations of the permeability values are higher than those of the separation factor and the ideal selectivity, because the former carries the uncertainty in the measurements of the film thickness, the flow rate, and the composition of the streams whereas the latter carries only the uncertainty in the gas composition measurement.

As seen in Table IV, the oxygen permeability coefficients of the EPMM1 and EPMM2 films decreased in comparison with that of the blank PPO film. An increase in the TEOS loading from 0 to 5% (PPO versus EPMM1) results in a decrease in the oxygen permeability coefficient by $\sim$ 19%. As the TEOS loading increases from 5 to 10% (EPMM1 versus EPMM2) the average oxygen permeability coefficient further decreases, however, this decrease is less the standard deviation values associated with the permeability coefficients. The results of X-ray diffraction analysis showed that a *d*-spacing of the films remained constant; however, the normalized peak intensity of the EPPM films indicated that they have lower crystallinity than the blank PPO film. In general, crystalline phases are impermeable and incapable of gas sorption, so their presence should lead to a decrease in the permeability to gases.[33] However, this description is not completely true for PPO. Alentiev et al.[34] reported that semicrystalline PPO and semicrystaline polydiphenyl-PPO are more permeable than and their amorphous copolymers, which is consistent with a higher permeability of semicrystalline PPO compared to that of amorphous EPMM films observed in the current study.

It is important to note that the EPMM1 film shows a higher separation factor and the ideal selectivity compared to PPO. Although this increase is just 8%, it is considerably greater than the standard deviation values associated with the measurements of the composition of the streams by the GC unit. On the other

TABLE IV
A Summary of Air Separation Tests Performed Using Blank PPO and EPMM Films

Film	Separation factor O_2/N_2	Ideal selectivity O_2/N_2	Permeability O_2 Barrer[a]	Permeability N_2 Barrer
Blank PPO				
Coupon 1	3.01 ± 0.003	4.249 ± 0.009	15.47 ± 1.44	3.64 ± 0.37
Coupon 2	3.00 ± 0.004	4.227 ± 0.010	15.51 ± 1.30	3.67 ± 0.35
EPMM1				
Coupon1	3.131 ± 0.004	4.557 ± 0.014	12.55 ± 1.02	2.75 ± 0.22
Coupon2	3.154 ± 0.007	4.605 ± 0.018	12.64 ± 1.03	2.74 ± 0.21
EPMM2				
Coupon1	2.695 ± 0.027	3.707 ± 0.037	12.02 ± 1.06	3.25 ± 0.28
Coupon2	2.721 ± 0.030	3.758 ± 0.044	12.12 ± 1.01	3.23 ± 0.25

[a] 1 Barrer = 10^{-10} cm^3(STP) × cm/(s × cm^2 × cmHg)

hand, EPMM2 film shows a lower separation factor and the ideal selectivity than PPO. A decrease in the ideal selectivity could indicate a beginning of phase separation. In turn, this would indicate that 10% of TEOS loading, which corresponds to 0.69% volume of the aqueous phase are the limiting values for the PPO-based EPMM membranes synthesized according to the procedure presented in this article.

The fact that EPMM films show selectivity in air separation indicates the absence of macrovoids in these films and hence a good compatibility between the nanoparticles and polymer chains. This is despite the presence of an aqueous phase in a highly hydrophobic medium of the PPO-TCE solution. Moreover, it should be emphasized that the tested films did not indicate any deterioration of their selective properties with time, which indicates their good mechanical integrity.

CONCLUSIONS

By performing the polycondensation of tetraethylorthosilicate (TEOS) in the presence of aluminum hydroxonitrate within the aqueous phase emulsified in a dilute solution of poly(2,6-dimethyl-1,4-phenylene oxide) (PPO) in trichloroethylene (TCE), we have demonstrated that it is possible to grow inorganic nanoparticles in a polymer matrix. The films prepared using the procedure described in this article can be referred to as EPMM films, and we have produced the EPMM films with an inorganic loading up to 10% based on the initial amount of TEOS. The presence of the particles measuring less than 1 μm in the cross section of the films was confirmed by the SEM analysis. In addition, the EDX analysis showed that the observed particles contained both Si and Al, thus confirming that TEOS had been hydrolyzed by aluminum hydroxonitrate. Moreover, the presence of inorganic components in the films was also confirmed by the TG analysis. The latter showed that the minimum conversion of TEOS, based on the mass balance of SiO_2, was 71.7%. The integrity of the EPMM films was confirmed in gas separation tests with air, in which the ideal selectivity for O_2/N_2 separation was observed to be as high as 4.6, which is 8% greater than the ideal selectivity of a blank PPO film. This indicates that PPO-based EPMM films have a great potential as gas separation membranes. The DSC analysis indicated that the glass transition temperature of the EPMM films strongly depends on the inorganic loading, i.e., the inorganic loading increases the glass transition temperature decreases. On the other hand, based on X-ray diffraction analysis, the inorganic loading does not significantly affect *d*-spacing of the EPMM materials. However, based on the normalized intensity of the major peak, the crystallinity of the films decreased slightly with inorganic loading.

The novel method of producing nanocomposite materials developed in this study could be employed to inorganic/polymer systems other than those considered in this work.

The authors would like to express their gratitude to Mr. Gilles P. Robertson from NRC for the thermogravimetric analysis and Dr. Lonardo Lastra from CANMET for SEM-EDX analysis.

References

1. Baker, R. W. Membrane Technology and Applications; Wiley, Hoboken, NJ, 2004.
2. Süer, M. G.; Bac, N.; Yilmaz, L. J Membr Sci 1994, 91, 77.
3. Jia, M.; Peinemann, K. V.; Behling, R. D. J Membr Sci 1993, 82, 15.
4. Mahajan, R.; Koros, W. J. Ind Eng Chem Res 2000, 39, 2692.
5. Smolders, C. A.; Duval, J. M.; Folkers, B.; Desgrandchamps, G.; Mulder, M. H. V. J Membr Sci 1993, 80, 189.
6. Chen, Y.; Iroh, J. O. Chem Mater 1998, 11, 1218.
7. Schaefer, D. W.; Mark, J. E. Polymer-Based Molecular Composites; Materials Research Society: Pittsburgh, PA, 1990; p 57.
8. Uragami, T.; Okazaki, K.; Matsugi, H.; Miyata, T. Macromolecules 2002, 35, 9156.
9. Jiang, R.; Kunz, H. R.; Fenton, J. M. J Membr Sci 2006, 272, 116.
10. Kusakabe, K.; Yoneshige, S.; Morooka, S. J Membr Sci 1998, 149, 29.
11. Nunes, S. P.; Peinemann, K. V.; Ohlrogge, K.; Alpers, A.; Keller, M.; Piers, A. T. N. J Membr Sci 1999, 157, 219.
12. Landry, C. J. T.; Coltrain, B. K.; Teegarden, D. M.; Long, T. E.; Long, V. K. Macromolecules 1996, 29, 4712.
13. Joly, C.; Goizet, S.; Schrotter, J. C.; Sanchez, J.; Escoubes, M. J Membr Sci 1997, 130, 63.
14. Schrotter, J. C.; Smaihi, M.; Guizard, C. J Appl Polym Sci 1996, 61, 2137.
15. Mascia, L.; Kioul, A. J Mater Sci Lett 1994, 13, 641.
16. Wu, C. M.; Xu, T. W.; Yang, W. H. J Membr Sci 2003, 216, 269.
17. Eliseev, A. A.; Kalinin, S. V.; Privalov, V. I.; Vertegel, A. A.; Tretyakov, Y. D. J Solid State Chem 1999, 147, 304.
18. Abismaïl, B.; Canselier, J. P.; Wilhelm, A. M.; Delmas, H.; Gourdon, C. Ultrason Sonochem 1999, 6, 75.
19. Dietz, W. A. J Gas Chromatogr 1967, 6, 68.
20. Crank, J. The Mathematics of Diffusion, 2nd ed.; Clarendo: Oxford, 1975.
21. Winstone, W. S.; Kamalesh, H.; Sirkar, K. Membrane Handbook; Van Nostrand Reinhold, New York, NY, 1992; Chapter 2, p 26.
22. Xie, Y. W.; Li, Y.; Ye, R. J Disp Sci Technol 2005, 26 455.
23. Behrend, O.; Ax, K.; Schubert, H. Ultrason Sonochem 2000, 7, 77.
24. Story, B.; Koros, W. J. J Membr Sci 1992, 67, 191.
25. Huang, Y. X.; Senos, A. M. R.; Rocha, J.; Baptista, J. L. J Mater Sci 1997, 32, 105.
26. Kim, J. H.; Lee, Y. M. J Membr Sci 2001, 193, 209.
27. Zhang, S.; Wu, C.; Xu, T.; Gong, M.; Xu, X. J Solid State Chem 2005, 178, 2292.
28. Wu, C.; Xu, T.; Yang, W. J Solid State Chem 2004, 177, 1660.
29. Kim, D. S.; Park, H. B.; Rhim, J. W.; Lee, Y. M. J Membr Sci 2004, 240, 37.
30. Karasz, F. E.; O'Reilly, J. M. J Polym Sci Polym Lett 1963, 3, 561.
31. Tran, A.; Kruczek, B. J Appl Polym Sci 2007, 106, 2140.
32. Wen, J.; Wikes, G. L. Chem Mater 1996, 8, 1667.
33. Micheals, A. S.; Bixler, H. J. J Polym Sci 1961, 50, 393.
34. Alentiev, A.; Drioli, E.; Gokzhaev, M.; Golemme, G.; Ilinich, G. O.; Lapkin, A.; Volkov, V.; Yampolskii, Y. J Membr Sci 1998, 138, 99.